Energetic Parameters Analysis of APFSDS Projectile Against Rolled Homogenous Armour For Enhanced Depth of Penetration

Quratulain[1], Adnan Tariq [1], Kamran Nazir [2], Umair Saleem [2] , Ali Raza [2,] *

[1] Mechanical Engineering Department, Wah Engineering College, University of Wah, Wah Cantt, Pakistan
[2] Mechanical Engineering Department, National University of Technology, Islamabad, Pakistan
* Correspondence: ali.raza@nutech.edu.pk

Highlights

- APFSDS
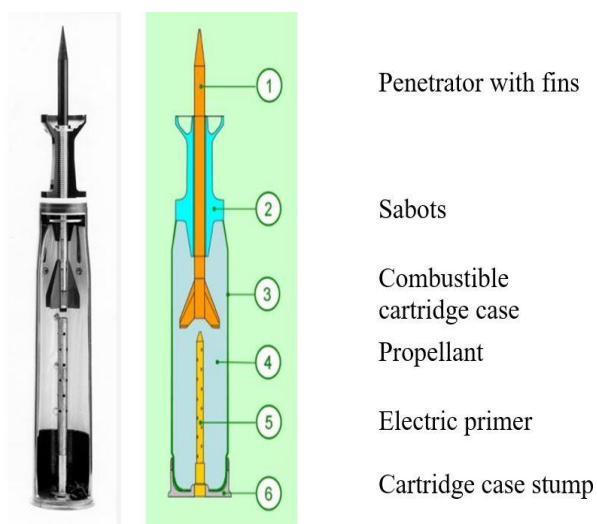- Projectile
- Explicit Dynamics

Abstract: Armor Piercing Fin Stabilized Discarding Sabot (APFSDS) is an anti-tank projectile, highly energetic for piercing armored vehicles. Its capability is measured against the depth it penetrates the standard target material. Terminal ballistics is the most important phase to analyze besides interior and exterior ballistics. With the improvements in armor materials, the depth it penetrates is a great concern. Research is available for different calibers projectile impact analysis taking one or some of the aspects using either empirical/numerical modelling or experimentation. This is a comprehensive research on a ballistic impact analysis of 125 mm caliber projectile addressing maximum aspects of the penetrator (Geometry, Density, Slenderness Ratio, Obliquity Angle, and Energetic Density) using real time limitations of firing system. Energetic parameters for 460 mm penetration experimentally, has been validated in Willi Odermatt (W-O) ballistic empirical model. Using this, different combinations of energetic parameters have been deduced against depth upto 700 mm. Moreover, experimental case energetic parameters have also been validated in numerical model using ANSYS Explicit Dynamics with Johnson Cook (J-C) Strength and Failure Model along with Mie-Grüneisen equation of state. Analysis showed that slenderness ratio of 25.12 is required for 700 mm penetration depth.

Keywords: Rolled Homogenous Armor; Ballistic Impact Analysis, Willi-Odermatt, Explicit Dynamics

1. Introduction

APFSDS that falls in Kinetic Energy Penetrators (KEPs) projectile as shown in Figure 1 is an anti-tank projectile which is used to fight the enemy armored fire assets. Short flying time i.e. 1.2 – 1.5 sec for 2000 meters, good hitting accuracy, significant penetration capability against RHA, lower susceptibility against interaction of reactive armour are its unique advantages.

1	Penetrator with fins
2	Sabots
3	Combustible cartridge case
4	Propellant
5	Electric primer
6	Cartridge case stump

Figure 1. APFSDS projectile (a: round, b: components)

Advancements in Kinetic Energy Penetrators (KEPs) occurred from earliest form i.e. cannon balls to the current modern, saboted penetrators with high slenderness ratio made of heavy strength and high-density metals with only goal to have high penetration capability against armoured vehicles [1]. KEPs do not have an explosive nature and the damage is caused by the kinetic energy imparted to the target. High muzzle velocity, heavy projectile, high aspect ratio rods provide KEPs high kinetic energy [2]. The impact of these projectiles is tested against benchmark materials like Rolled Homogenous Armour (RHA).

Flight of an APFSDS projectile has four stages; internal ballistics, intermediate ballistics, external ballistics and terminal ballistics as shown in Figure 2 [3, 4]. Efficiency of APFSDS projectile is principally related to the terminal ballistic performance besides other parameters.
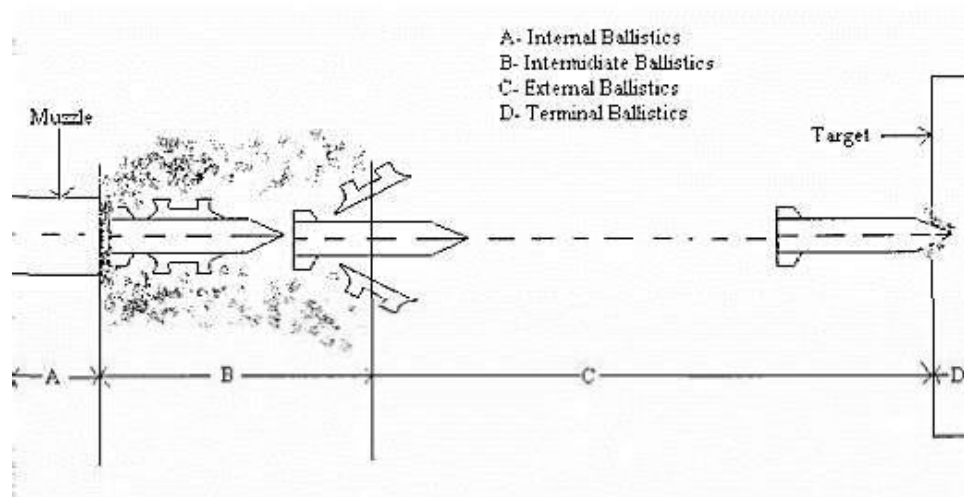
Figure 2. Ballistic stages of APFSDS flight

Ballistic impact analysis of projectiles with different calibers has remained an area of interest. Several authors worked to capture impact phenomenon of small caliber projectiles while significant literature is also available where artillery caliber of projectile is under consideration to analyze its behavior at the time of impact [5-7]. Literature shows that ballistics impact analysis has been carried out considering one or multiple aspects of projectile which includes its geometry, density, slenderness ratio, energetic density or obliquity angle. Zaki

et al [8] carried out impact analysis of Tungsten Heavy Alloy (WHA) long rod with same density and has assessed projectile penetration efficiency by varying slenderness ratio only. Approach followed for impact analyses includes Alekseev ski- Tate empirical model and have compared results with experimental data. Li et al [9] has carried out impact analysis varying material of penetrator consequently varying densities. Due to high plasticity inherent in WHA material, comparative simulations were performed to simulate impact behavior of composite rod made of Tungsten Particle/ Metallic Glass (WP/MG) matrix and Tungsten Fiber/ Metallic Glass (WF/MG) matrix. The work on simulations was integrated with related experimental investigations.

Impact analysis performed by Yoo et al [10] considers obliquity angle and different geometries of projectile. He developed simulation model with finite cavity method and verified that model based on previous experiments. Further he performed comparative assessment for depth of penetration with different geometry and obliquity angle. Magier [11] research on ballistic impact involves experimentation approach. He presented basic energetic parameters of selected 120 mm APFSDS in service projectiles followed by their analyses and hypothetical projectile recommendation with estimated chances for meeting penetration capacity of one meter through RHA at distance of two meters. Besides factor that effect penetration significantly which are impact velocity, penetrator material, slenderness ratio, Magier research incorporates energetic density of projectile penetrator. Energetic density is a basic parameter which indicates capacity of projectile for penetrating the armor.

Similarly, research on impact analysis carried out by Akella [12], Mubashar et al [13] and Roy et al [14] involves varying geometry of projectile whereas Banerjee et al [15], Borvik et al [16-18], Bhuarya et al [19] and Yaziv et al [20] performed impact analysis of projectile at varying obliquity angles in addition to varying geometries. Selected target material for impact analysis can be aluminium, ceramic, steel as per projectile calibre and material. Few authors expressed design limitations due to firing system [11, 21]. One or combination of different approaches i.e. empirical modelling, numerical modelling, direct experimentation followed by researches are found in literature. Advancements have been made in design of APFSDS with one goal of achieving enhanced depth of penetration. Firing an APFSDS is not simple; first the target has to be acquired and the process of carrying the penetrator to target goes through the four complicated stages of ballistics with their own sets of engineering problems. With the advancements in the material of armor, terminal ballistics phase draws more attention compared to intermediate and internal ballistics. Mathematical models for impact mechanics have been greatly improved over time from Newton's simplified understanding of impact mechanics to modified empirical models as presented by Willi Odermatt. These models being empirical in nature do not generate strain, stress or wave propagation as outputs. With the advancements in FEM, newer models have developed. Explicit dynamics are extensively used for impact analysis that covers non linearity of material. To simulate the impact of an APFSDS, AUTODYN is used with appropriate material properties. Mathematical model capable to evaluate stress, strain rates along with the thermal softening effects is required. J-C strength and failure model serves the purpose and captures strain rate sensitivity of the materials appropriately. The hydrostatic pressure, the local density, and local specific energy is related using Mie-Gruneisen equation of state in numerical analysis.

The geometrical parameters of penetrators along with the obliquity angle and energetic density have influential effect in the penetration of kinetic energy projectiles. The aim of this study is to evaluate their effects in designing of kinetic energy projectiles with an improved penetration, considering the limitations of firing

system. Methodology followed for research includes validation of experimental results with empirical model through MATLAB as well as with numerical code through ANSYS. Further, empirical model has been utilized to extract design points for enhanced penetration from 550 - 700 mm with an interval of 50 mm and their evaluation in numerical code of ANSYS to visualize penetration at enhanced depths.

2. Experimental Design & Validation

Figure 3 shows penetrator design of experimental case that gives penetration of 460 mm in RHA target. Obliquity angle is kept 53º for this design. Table 1 contains geometrical parameters whereas mechanical properties are provided in Table 2.
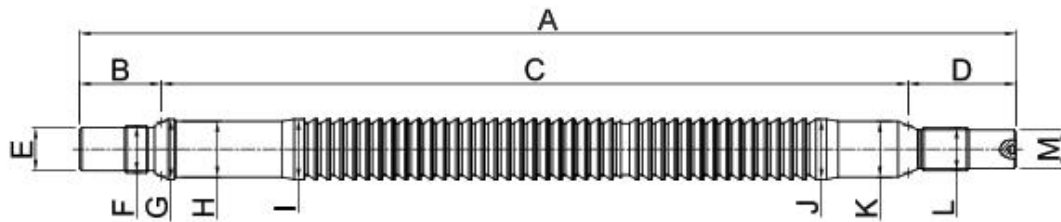
Figure 3. APFSDS projectile's penetrator (experimental design)

Table 1. Geometrical parameters

Property	Value
Penetrator	
A: Total Length	437 mm
B: Length	38 mm
C: Length	349 mm
D: Length	50 mm
E, L: Diameter	20 mm
F: Diameter	22 mm
G, I,J: Diameter (max)	28 mm
H,K: Diameter(plain)	26 mm
M: Diameter	18 mm
Target Plate	
Thickness	275 mm
Cross-sectional Area	5 x 5 ft^2

Table 2. Mechanical Properties

Property	Penetrator	Target Plate
Mass	3.685 kg	-
Yield Stress	1400 MPa	820 MPa
Density	17126 kg/m^3	780 kg/m^3
Hardness	466	223

2.1. Validation in Empirical Model

An empirical relationship for the perforation limit of kinetic energy APFSDS rounds is deduced by Willi Odermatt as in (1) with analytical constraints fitted for experimental data for approximately 74 tests. There is a great correspondence between the model and experimental data with maximum difference of 6%.

$$\frac{d}{D} = a\left(\frac{L}{D}\right).(cos\theta)^m.\sqrt{\frac{\rho_P}{\rho_T}}.e^{\frac{-c.R_m}{\rho_P.v_T^2}} \tag{1}$$

$$\text{T1} \qquad \text{T2} \qquad \text{T3} \qquad \text{T4}$$

Where:

$$a\left(\frac{L}{D}\right) = \left(\frac{L}{D}\right) + 3.94.\left(1 - \tanh\frac{\frac{L}{D} - 10}{11.2}\right)$$

$$c = 22.1 + 1.27e^{-8}R_m - 9.47e^{-18}R_m^2$$

$$m = 0.775$$

Term T1 represents length to diameter ratio, T2 target obliquity, T3 density ratio of penetrator to target and T4 represents material properties and incident velocity. Empirical model established by Willi Odermatt was modelled in MATLAB to validate existing design of APFSDS projectile explained in section II.

According to MATLAB calculations, the experimental design of penetrator gives 458.4 mm penetration depth. This penetration depth in comparison with 460 mm as in experimental case differs with only 0.35 % which is well within the allowable difference of 6%.

2.2. Validation in Numerical Model

Experimental parameters have been replicated using the material constants listed by the authors and available material properties of penetrator and target material. The impact analysis was carried out in ANSYS Explicit Dynamics with AUTODYN solver.

2.2.1. Material Properties

The material properties necessary for a J-C model for both penetrator and target material are given in Table III and Table IV. Penetrator material corresponds to tungsten alloy and target material corresponds to RHA steel.

These properties have been confirmed through the simulations in AUTODYN solver of Explicit Dynamics module (ANSYS Workbench). Damage and failure criteria for RHA plate was defined by J-C damage model.

Table 3. Material Properties of Target (Rha)

Properties	Values
Density	7860 kg/m³
Yield Strength	820 MPa
Shear Modulus	64100 MPa
Reference Strain Rate	1 s⁻¹

Melting Temperature	1700.2 K
Grüneisen Coefficient	1.67
Parameter C1	4610 ms^{-1}
Parameter S1	1.73
Parameter Quadratic S2	0 ms^{-1}
Damage Constant D1	0.05
Damage Constant D2	3.44
Damage Constant D3	-2.12
Damage Constant D4	0.002
Damage Constant D5	0.61

Table 4. Material Properties of Penetrator (Tungsten Alloy)

Properties	**Values**
Density	17126 kg/m^3
Specific Heat	134 Jkg^{-1} C^{-1}
Initial Yield Stress	1400 MPa
Hardening Constant	1057 MPa
Hardening Exponent	0.6125
Strain Rate Constant	0.02247
Thermal softening exponent	1
Melting Temperature	1700.2 K
Shear Modulus	1.6x10^5 MPa
Grüneisen Coefficient	1.54
Parameter C1	4029
Parameter S1	1.237
Parameter Quadratic S2	0 ms^{-1}

2.2.2.   Geometry Formulation

The main factors that control the depth of penetration are the working aspect ratio and material properties, so, a simplified model comprising of 2-dimensional, axisymmetric model with a rectangular computational domain of uniform mesh resolution throughout was prepared using Design Modeler included in ANSYS Workbench as per experimental based design of APFSDS projectile. Geometry formulated in ANSYS Design Modular is shown in Figure 4. Computational domain sizes kept for penetrator and target plate are provided in Table 5.
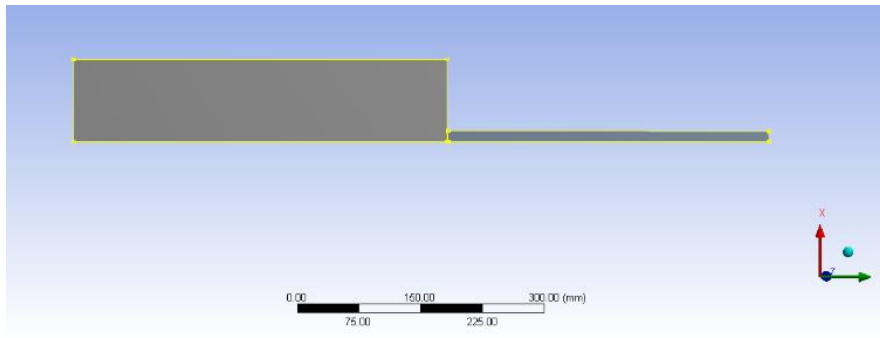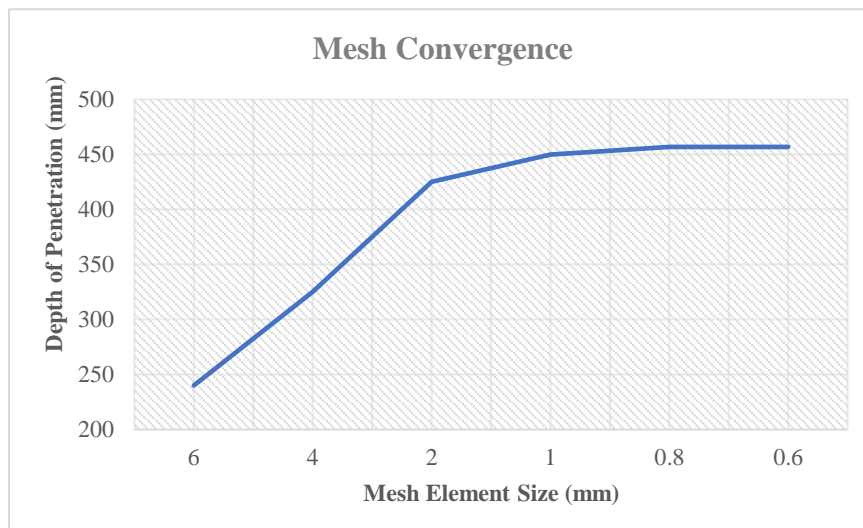
Figure 4. Geometry for experimental based design of APFSDS projectile

Table 5. Geometrical parameters used in numerical model

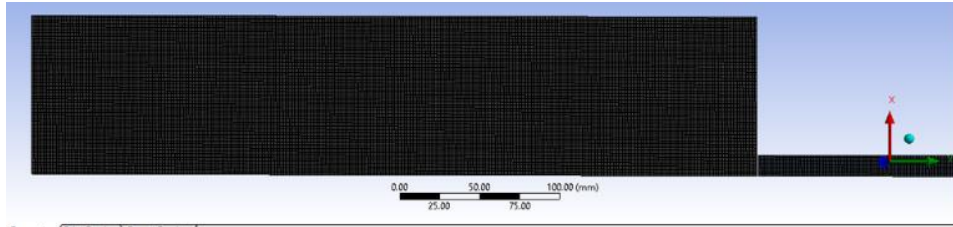| Property	Value
Penetrator	
Length (effective)	395 mm
Diameter (plain)	26 mm
Slenderness Ratio	15.19
Target Plate	
Thickness	700 mm
Height	200 mm

2.2.3. Meshing

Mesh convergence check was performed to determine the optimum number of mesh element size required to use less computational power without any compromise on accuracy of results. Mesh element with size of 0.8 mm both for penetrator and RHA plate (number of elements i.e., 120,000 approx.) gave satisfied result as shown in Figure 5. To greatly improve solution time and the meshing so that errors such as 'time step is too low' and 'energy error is too high' do not occur, structured meshing is used. Meshing size is also finer with mesh element size of 0.8 mm, to capture the effect of "mushrooming".

Figure 5. Mesh convergence

Mesh and Mesh statistics for experimental based design of APFSDS projectile are shown in **Error! Reference source not found.** and in Table 6.

**Figure 6.** Mesh design of APFSDS projectile

Table 6. Mesh Statistics for Experimental Based Design

Properties	Value
Element size	0.8 mm
Nodes	118791
Elements	117279
Orthogonal Quality	1
Skewness	1.3e-10
Aspect Ratio	1.0011

2.2.4. Solution

The muzzle velocity and internal ballistics are same therefore constant impact velocity i.e. 1595 m/s is considered. Fixed support condition was employed at the side of target plate.

The depth of penetration predicted by the finite element model is 462 mm while that obtained in experiment is 460 mm Figure 6. The difference in this value with respect to the experimental value is 0.4 %. The results are in good agreement.
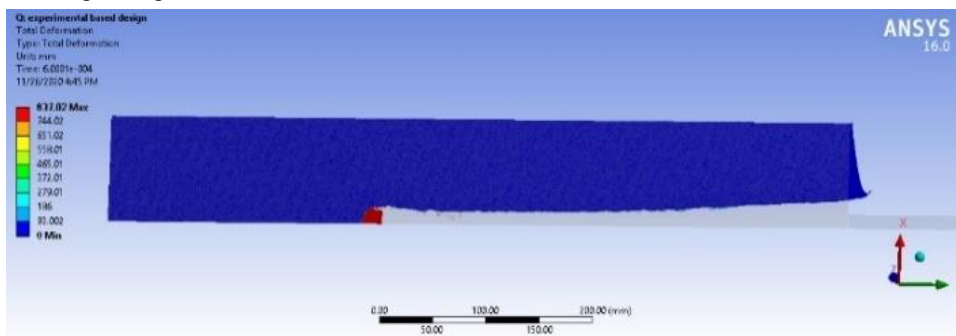
Figure 6. Penetration of experimental based design (462 mm)

Other than the material properties, certain necessary phenomenon like shear banding/adiabatic shearing, "mushrooming" was also observed to verify that the J-C Model was predicting these phenomenon

as it should as shown in Figure 7. Therefore, damage pattern at the end of simulation also matches with experimental results.
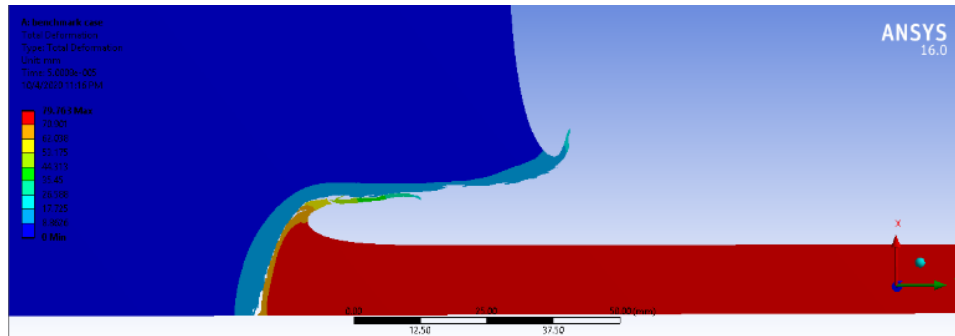

Figure 7. Mushrooming effect at 50 microseconds

3. **Analysis of Energetic Parameters**

3.1. Obliquity angle

In general, penetration of projectiles is made at some oblique angle compared to normal penetration. Target plate used in this research has constant thickness of 275 mm. The relationship between obliquity angle and desired penetration with constant thickness target plate is provided in Figure 9 using MATLAB.
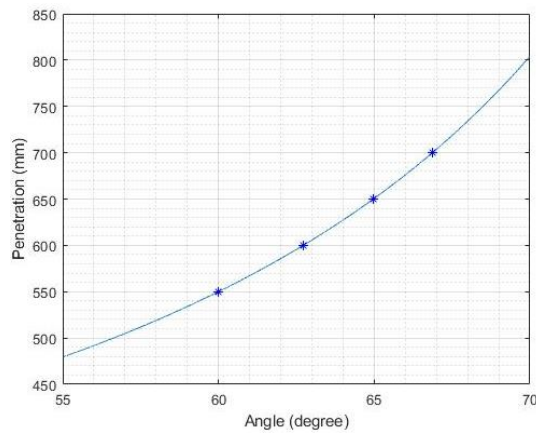

Figure 8. Obliquity angle and penetration depth with constant thickness target plate

3.2. Effective Length of Penetrator

To see the effect of effective length of penetrator with depth of penetration, length of penetrator is varied from 400 mm to 650 mm with constant diameter. Solving in MATLAB provides linear relationship for penetrator length with depth of penetration as shown in Figure 9 and Figure 10 also shows linear relationship of depth of penetration for increasing slenderness ratios at constant diameter.
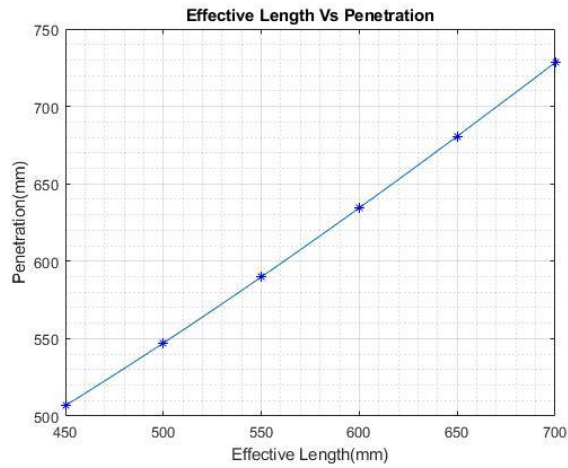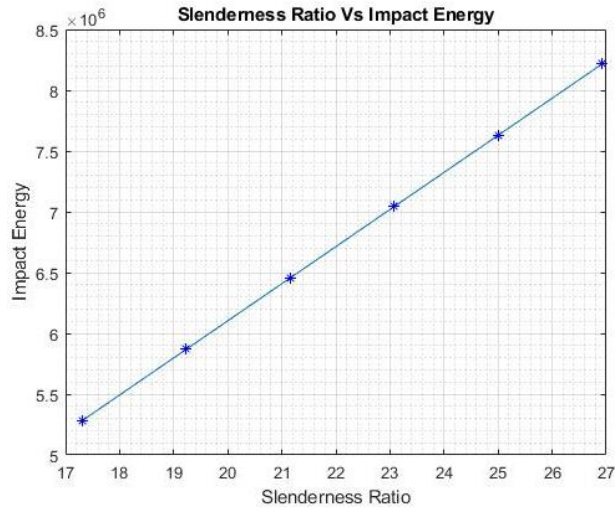
Figure 9. Depth of penetration at verying length and constant diameter
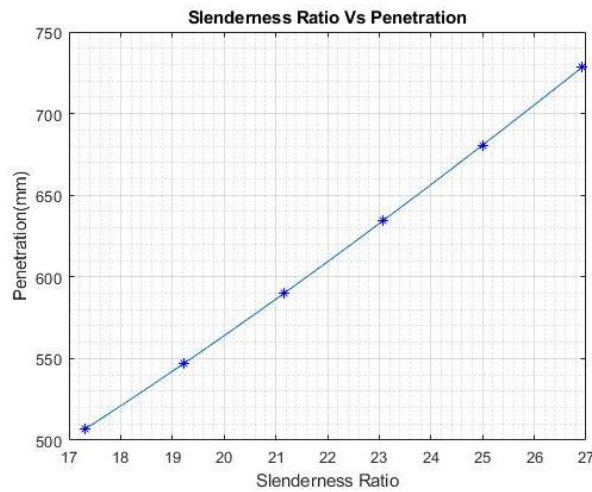
Figure 10. Variation in depth of penetration at different slenderness ratio

(varying length & constant diameter)

Based on this volume and length dependence, the mass also changes accordingly. Therefore, the impact energy shows a similar trend as in Figure 11.

Figure 11. Impact energy at different slenderness ratio (varying length & constant diameter)

By changing effective length of penetrator, slenderness ratio changes from say 19-20 for only a linear change of roughly 0.2 MJ.

3.3. Diameter of Penetrator

Study comprising of varying diameters of penetrator and constant length was also carried out in MATLAB to assess the effect of diameter on depth of penetration. Graphical trend shows negative slope for slenderness ratio for increasing diameters as shown in Figure 12 and negative slop for depth of penetration at increasing slenderness ratio as shown in   Figure 13.
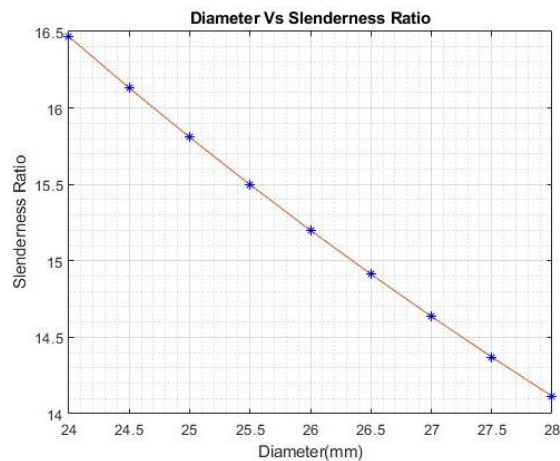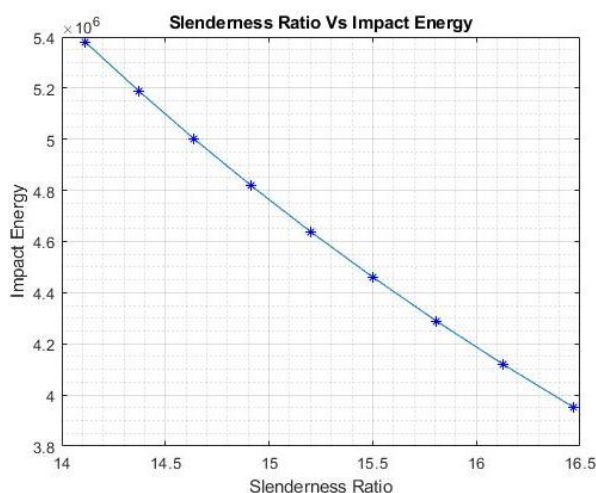

Figure 12. Slenderness ratio at varying diameters (constant length)
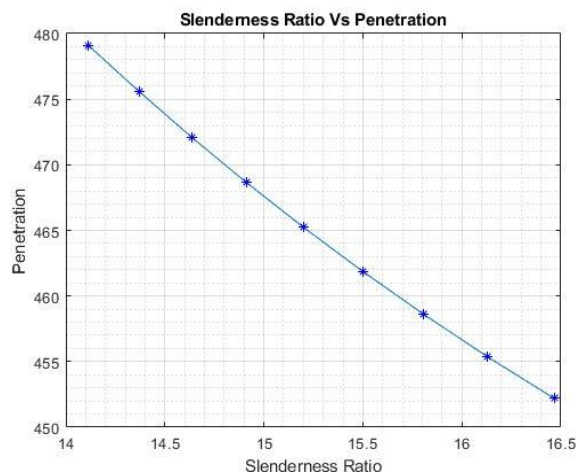
**Figure 13.** Depth of penetration at various slenderness ratios (varying diameter and constant length)

This is the case because although for L/D of 16.5, the diameter is only 24 mm and the mass and impact energy are not enough to penetrate to a greater depth. Diameter variation is quadratic in nature and consequently so is the change in mass and impact energy as shown in Figure 14.

Figure 14. Impact energy at different slenderness ratios (varying diameter and constant length)

3.4. Slenderness Ratio of Penetrator

Comprehensive representation is required to show the effect of slenderness ratio on penetration that should also take into account varied length and diameter. Figure 15 serves the purpose. It shows a detailed graphical representation of slenderness ratios and depth of penetration for different combinations of length and diameters. Length is from 400 mm to 650 mm with twenty equal intervals. Similarly, diameter is varied from 24 mm to 28 mm with nine equal intervals. Design points for desired depth of penetration can be taken from this figure in terms of length, diameter and slenderness ratio of penetrator.
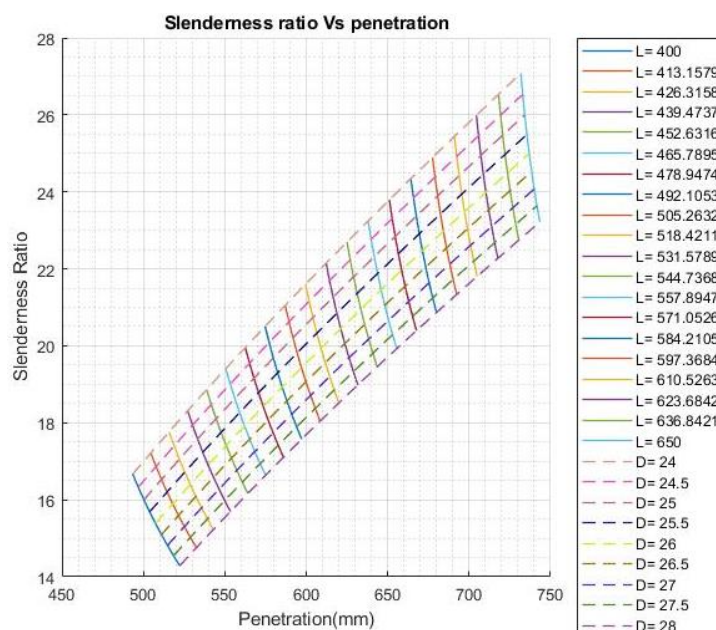
Figure 15. Slenderness ratio at different depths of penetration (varying length and diameter)

With the increase in penetrator effective length from 400 mm to 650 mm, depth of penetration is increasing from 490 mm to 740 mm. Similarly change in diameter can be related in terms of aspect ratio. For decreasing diameter i.e. 28 mm to 24 mm, aspect ratios are increasing from 14 to 17 at min length of 400 mm and from 23 to 27 at max length of 650 mm. With the increase in aspect ratio, increase in penetration depths can be seen.

Here these design points are valid if condition for constant mass, varying obliquity angle are not considered. Slenderness ratio achieved so far is 30.

3.5. Energetic Density

It is commonly accepted that a basic parameter indicating capacity for penetrating the armour at the time of impact is energetic density (ED). It is given by the equation (2) and (3):-

$$GE = \frac{2mV^2}{\pi d_w^2} \tag{2}$$

Where GE: energetic density of projectile's penetrator (kJ/mm2), m: mass of penetrator (kg), V: penetrator hitting velocity into armor (m/s), d_w: diameter of penetrating crater (mm)

$$d_w = d + \Delta d \tag{3}$$

Where d: diameter of penetrator, $\Delta d \approx 0.1d$ (in practice it is assumed ($1 \leq \Delta d \leq 3$) mm.

Modelling equation for energetic density in MATLAB, we get quadratic relation of diameter and energetic density with a negative slope as shown in Figure 16. It suggests keeping diameter minimum for large energetic density and ultimately increasing penetration capability of KEPs.
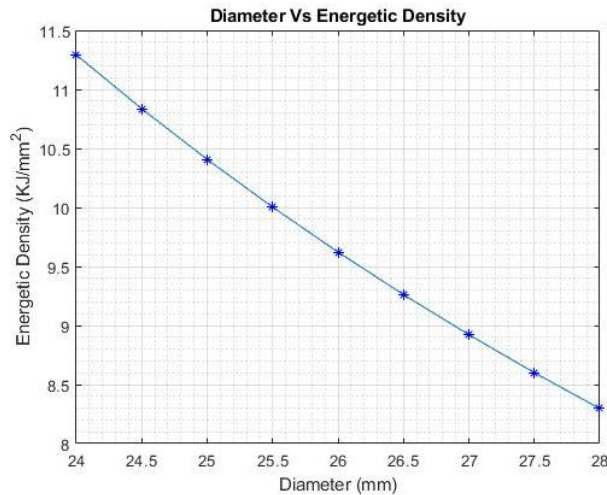
**Figure 16.** Energetic density of penetrator at different diameters

4. Design Points Determination and Evaluation for Enhanced Depth of Penetration

Characteristics of penetrator addressing design limitations offered by firing system, conventional propellant and machining constraints are tabulated in Table 7 below: -

Table 7. Design Parameters of KEPS

Parameter	Value
Mass (kg)	3.6 - 4.86
Diameter (mm)	24 -28
Length (mm)	400-650
Muzzle velocity (m/s)	1750 max
Impact velocity (m/s)	1595 min
Density (kg/m^3)	17.126 – 17.380

Addressing mass of the penetrator i.e. 4.86 kg and obliquity angle for 275 mm thick target plate we get graphical representation between slenderness ratio and depth of penetration as shown in Figure 17 and Figure 18 shows results obtained considering constant mass and obliquity angle required for 275 mm thick RHA plate.
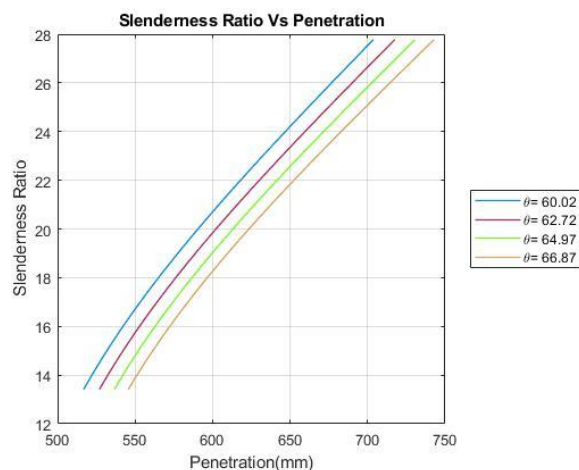
Figure 17. Slenderness ratio and penetration addressing mass and obliquity angle
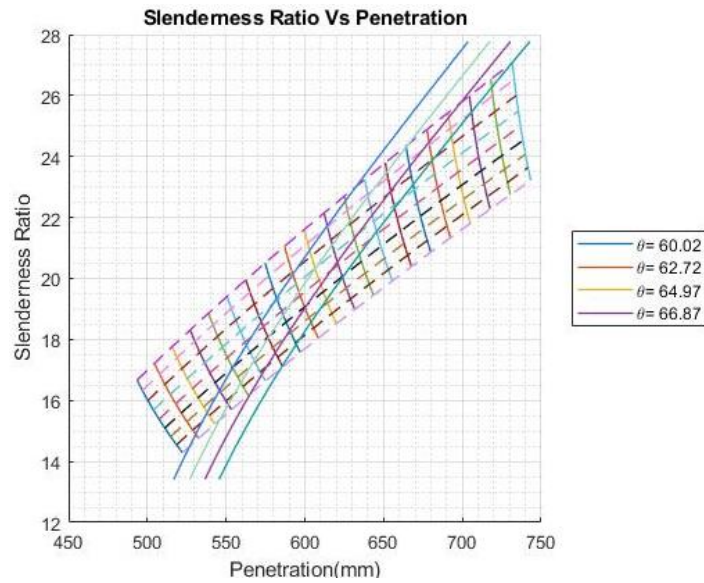
Figure 18. Slenderness ratio and penetration considering constant mass and obliquity angle

From the above graph design points in terms of slenderness ratio at different depths of penetration can be extracted.   These are provided in Table 8.

Table 8. Selected design points at different depth of penetration

Design Point	Penetration (mm)	Slenderness Ratio	Length (mm)	Diameter (mm)
DP 1	550	16.75	464	27.7
DP 2	600	19.85	520	26.2
DP 3	650	22.55	566	25.1
DP 4	700	25.12	608	24.2

Design points achieved have been evaluated in ANSYS to predict impact phenomenon.   Parametric simulations of design points have been performed by applying a common set of characteristics in all simulations including J-C strength and failure model. Depth of penetration achieved against each design point is provided in Table 9 Figure 19.

Table 9. Depth of penetration achieved at design points in numerical modeling

Design Point	Penetration (mm)
DP 1 @550 mm	552
DP 2 @600 mm	618
DP 3 @650 mm	670
DP 4 @700 mm	715

DP 1 @550 mm: Penetration of 464/27.7 Penetrator (P=552 mm)

DP 2 @600 mm: Penetration of 520/26.2 Penetrator (P=618 mm)

DP 3 @650 mm: Penetration of 566/25.1 Penetrator (P=670 mm)

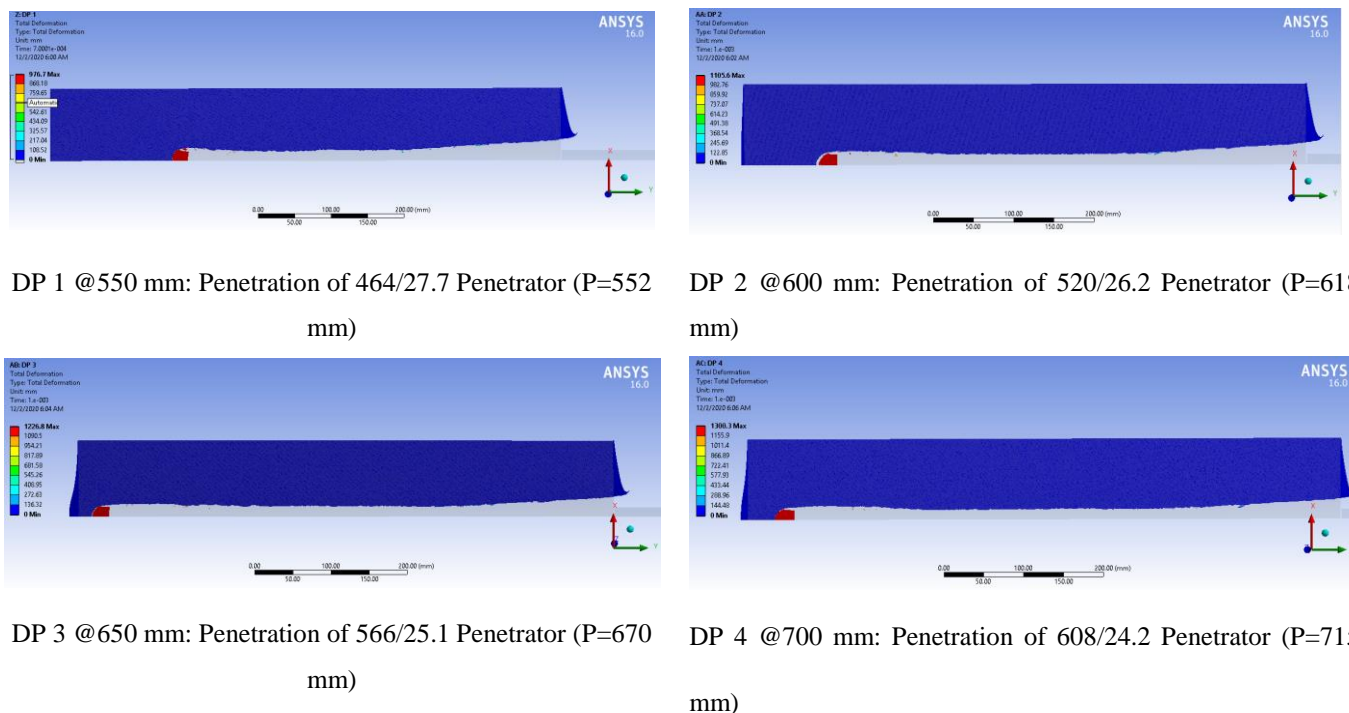DP 4 @700 mm: Penetration of 608/24.2 Penetrator (P=715 mm)

Figure 19. Depth of penetration achieved at design points in numerical modeling

5. Conclusion

An APFSDS projectile is used for piercing armored vehicles. Its lethality is tested against benchmark target material like Rolled Homogenous Armor (RHA). Predicting the penetration depth of the projectile is one of the essential aspects of projectile design. In this study, an experimental case has been validated to verify the modelling approach using W-O ballistic empirical model and FEM based numerical model. Experimental case has 460 mm depth of penetration against RHA target. Depth of penetration achieved through W-O ballistic model is 458.4 mm with a difference of 0.35 % only. However, Willi Odermatt ballistic model allows error limit up to 6%. The difference obtained in FEM simulations is 0.4% only with penetration depth of 462 mm. Empirical model is inferior as J-C strength model takes into consideration stress, strain rates and temperature (thermal softening). Therefore, results obtained through FEM simulations are closer to reality.

The next phase of research is to evaluate design parameters that effects depth of penetration of APFSDS projectile on RHA target significantly. The correlation of design parameters of penetrator (obliquity angle, effective length, diameter, slenderness ratio, energetic density) with depth of penetration has been evaluated in detail in section III. Keeping all factors into account design points at four depth of penetration i.e., 550 mm, 600 mm, 650 mm and 700 mm have been obtained from empirical model followed by simulation of all points in ANSYS. Comparison of results obtained from both models are shown in Table 10 and Figure 20.

Table 10. Comparison of penetration depths obtained by W-O model and J-C model

Design Point	Slenderness Ratio	Length (mm)	Diameter (mm)	Penetration (mm)		% Age Difference
				W-O Model	**J-C Model**	
DP 1	16.75	464	27.7	550	552	**0.40**
DP 2	19.85	520	26.2	600	618	**3.0**

DP 3	22.55	566	25.1	650	670	**3.1**
DP 4	25.12	608	24.2	700	715	**2.14**
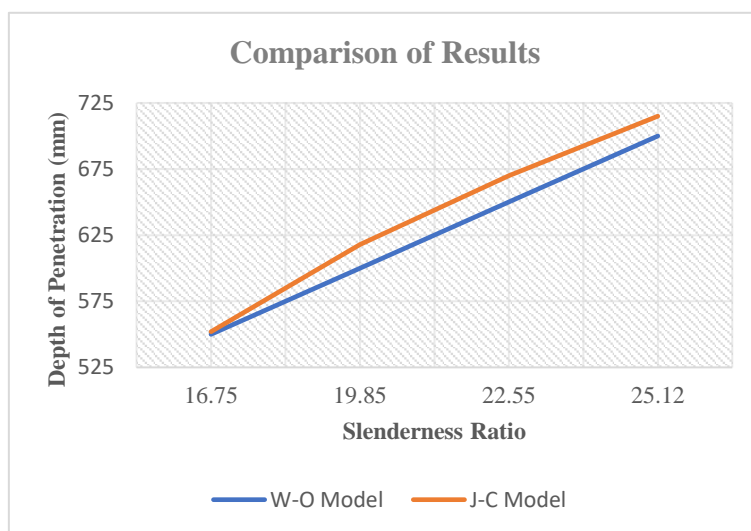
Figure 20. Comparison of penetration depths obtained by W-O model and J-C model

It can be concluded with increase in slenderness ratio of penetrator, depth of penetration is increasing. Moreover, J-C model predicts better behavior at impact as it involves stress, strain rates and temperature (thermal softening effects). To ensure accuracy of results mesh convergence check has been performed and mesh element size of 0.8 mm for both penetrator and target plate was found.

Shear banding/adiabatic shearing, "mushrooming" effect was also observed in finer mesh which verify that the J-C is predicting the impact phenomenon as it should. Other than mushrooming, some failed material can also be seen spewing out of the hole. Most of the failed mesh is removed on failure and erosion to help with visually identifying the penetration length.

References

[1]   W. Lanz, W. Odermatt, and G. Weihrauch, "Kinetic energy projectiles: development history, state of the art, trends," in *19th International Symposium on Ballistics (Interlaken, Switzerland, 7–11 May 2001)*, 2001, pp. 1191-1197.

[2]   B. P. Burns, W. H. Drysdale, C. P. Hoppel, and T. A. Bogetti, "The Development of Composite Sabots for Kinetic Energy Projectiles," *US Army,* vol. 1500, pp. 21005-5066, 2001.

[3]   E. W. Lach, "Ballistics–experiments and modelling."

[4]   N. P. N.Eches, C. DoffŽ mont; Giat Industries,, "In bore behaviour of large calibre armour piercing fin stabilised discarding sabot ".

[5]   G.-F. GAO, Y.-C. LI, R.-Y. HUANG, and S.-W. DUAN, "Study on Effect Mechanism of Aspect Ratio for Vertical Penetration of a Long-Rod Projectile," *Chinese Journal of High Pressure Physics,* p. 7, 2011.

[6]   J. H. Joo, C. H. Lee, and J. H. Choi, "A Numerical Research on the Penetration into a Semi-Infinite Rolled Homogeneous Armor by a Medium-Caliber Kinetic Energy Projectile," in *Materials Science Forum*, 2011, pp. 197-202.

[7]   S. J. Schraml, "Constitutive model parameter study for armor steel and tungsten alloys," in *Dynamic Behavior of Materials, Volume 1*, ed: Springer, 2011, pp. 409-418.

[8]   S. Zaki, E. Uddin, and A. Mubashar, "Experimental investigation of impact of long rod eroding projectiles against rolled homogeneous armour," *Proceedings of the Institution of Mechanical Engineers, Part L: Journal of Materials: Design and Applications,* vol. 234, pp. 1335-1342, 2020.

[9]   J.-c. Li, X.-w. Chen, and F.-l. Huang, "Ballistic performance of tungsten particle/metallic glass matrix composite long rod," *Defence Technology,* vol. 15, pp. 132-145, 2019.

[10]   Y.-H. Yoo, J.-B. Kim, and C.-W. Lee, "Effects of the Projectile Geometries on Normal and Oblique Penetration Using the Finite Cavity Pressure Method," *Applied Sciences,* vol. 9, p. 3939, 2019.

[11]   M. Magier, "Analiza parametrów energetycznych przeciwpancernej amunicji podkalibrowej w aspekcie oczekiwań współczesnego pola walki," *Problemy Techniki Uzbrojenia,* vol. 46, 2017.

[12]   K. Akella, "Studies for improved damage tolerance of ceramics against ballistic impact using layers," *Procedia engineering,* vol. 173, pp. 244-250, 2017.

[13]   A. Mubashar, E. Uddin, S. Anwar, N. Arif, S. Waheed Ul Haq, and M. Chowdhury, "Ballistic response of 12.7 mm armour piercing projectile against perforated armour developed from structural steel," *Proceedings of the Institution of Mechanical Engineers, Part L: Journal of Materials: Design and Applications,* vol. 233, pp. 1993-2005, 2019.

[14]   S. K. Roy, M. Trabia, B. O'Toole, R. Hixson, S. Becker, M. Pena, *et al.*, "Study of hypervelocity projectile impact on thick metal plates," *Shock and Vibration,* vol. 2016, 2016.

[15]   A. Banerjee, S. Dhar, S. Acharyya, D. Datta, and N. Nayak, "Determination of Johnson cook material and failure model constants and numerical modelling of Charpy impact test of armour steel," *Materials Science and Engineering: A,* vol. 640, pp. 200-209, 2015.

[16]   T. Børvik, A. H. Clausen, O. S. Hopperstad, and M. Langseth, "Perforation of AA5083-H116 aluminium plates with conical-nose steel projectiles—experimental study," *International Journal of Impact Engineering,* vol. 30, pp. 367-384, 2004.

[17]   T. Børvik, M. Forrestal, O. Hopperstad, T. Warren, and M. Langseth, "Perforation of AA5083-H116 aluminium plates with conical-nose steel projectiles–calculations," *International Journal of Impact Engineering,* vol. 36, pp. 426-437, 2009.

[18]   T. Børvik, L. Olovsson, S. Dey, and M. Langseth, "Normal and oblique impact of small arms bullets on AA6082-T4 aluminium protective plates," *International Journal of Impact Engineering,* vol. 38, pp. 577-589, 2011.

[19]   M. K. Bhuarya, M. S. Rajput, and A. Gupta, "Finite element simulation of impact on metal plate," *Procedia Eng,* vol. 173, pp. 259-263, 2017.

[20]   D. Yaziv, M. Mayseless, and Y. Reifen, "The penetration process of long rods into thin metallic targets at high obliquity," in *Proc. 19th Int. Symp. On Ballistics. Interlaken, Switzerland*, 2001, pp. 1257-1264.

[21]   S. Baloš, M. Nikačević, P. Ristić, and L. Šiđanin, "Jacketed long-rod penetrators: Problems and perspectives," *Scientific Technical Review,* vol. 60, pp. 70-75, 2010.